Ferromagnetic resonance and spin wave resonance in multiphase materials: theoretical considerations

1998 J. Phys.: Condens. Matter 10 10679

(http://iopscience.iop.org/0953-8984/10/47/018)

J. Phys.: Condens. Matter **10** (1998) 10679–10700. Printed in the UK PII: S0953-8984(98)93705-5

Ferromagnetic resonance and spin wave resonance in multiphase materials: theoretical considerations

D S Schmool† and J M Barandiarán

Departamento de Electricidad y Electrónica, Facultad de Ciencias, Universidad del País Vasco/EHU, Apartado 644, 48080 Bilbao, Spain

Received 28 April 1998, in final form 24 August 1998

Abstract. The theory of ferromagnetic resonance (FMR) and spin wave resonance (SWR) is presented for the general case of multiphase ferromagnets. This could be a magnetic multilayer structure or a material with mixed phases of distinct ferromagnetic materials. We discuss the application of the theory to various systems, with a description of amorphous and nanocrystalline materials which have not received much attention with respect to FMR and SWR. In this respect, we treat these materials in a multiphase manner for the first time, where previous FMR measurements on these types of material have been analysed and interpreted as single phase ferromagnets. Although the general theory is applicable to an N phase material, we show the detailed analysis for two phase systems, giving examples of both magnetic multilayers and mixed double phase ferromagnets of the type for mixed nanocrystalline and amorphous magnetic systems. The theory would also be applicable to systems where a magnetic phase is surrounded by a non-magnetic phase, such as co-deposited systems. We also consider, for the first time, the possibility of the existence of standing spin wave modes in mixed phase and granular materials. The adaptability of the general theory to any form of magnetocrystalline anisotropy and interphase interaction is also discussed.

1. Introduction

Materials of mixed magnetic phases have been of very significant scientific interest in recent years, whether they be in the form of magnetic multilayered structures [1–4], or randomly distributed, as in systems of amorphous and nanocrystalline mixed phase alloys [5–8]. These materials offer a new range of magnetic properties making them technologically very important. Such properties can be obtained by combining the differing characteristics of various magnetic materials and/or by exploiting the varying magnetic interphase exchange coupling interaction. In all mixed magnetic phase systems, the exchange coupling interaction between magnetic phases plays a vital role in the 'global' magnetic properties exhibited by these materials. In the field of magnetic multilayers there has been very extensive research which has shown that the magnetization vectors between adjacent layers can couple ferromagnetically, antiferromagnetically [2–4, 9, 10] and in some cases perpendicularly (biquadratic coupling) [11, 12]. The form of the coupling is dependent on the interlayer material, crystallographic structure and orientation as well as the thickness. Many authors have attributed the observed oscillatory coupling (from

† Corresponding author/present address: Laboratoire de Magnétisme et d'Optique, Université de Versailles, CNRS, 45 Avenue des Etats-Unis, 78035 Versailles, France. E-mail address: dschmool@physique.uvsq.fr.

0953-8984/98/4710679+22$19.50

ferromagnetic to antiferromagnetic alignment), as a function of the interlayer thickness, to an RKKY type interaction between the ferromagnetic layers through the non-magnetic interlayer [13–15]. For the amorphous and nanocrystalline mixed systems, the exchange interaction acting between the nanocrystallites through the intervening amorphous magnetic phase is responsible for the very soft magnetic properties exhibited by these types of material [7, 8].

Microwave spectroscopy, in the form of ferromagnetic resonance (FMR) and spin wave resonance (SWR), has been demonstrated to be a very powerful probe of the magnetic properties of many types of magnetic material. For example, we can obtain information on the bulk magnetic properties of materials, such as the saturation magnetization, magnetocrystalline anisotropies and g-factors. In the case of magnetic confinement effects, we can further deduce microscopic quantities such as the exchange stiffness constant by spin wave resonance. With careful analysis, we can study properties of grains and thin films, where linewidth broadening can give information on interfacial roughness and grain sizes. From the nature of spin wave resonance spectra, i.e. field position and intensities of resonance lines, we can infer surface anisotropies of magnetic films. FMR/SWR has been applied to the study of both magnetic multilayer [16–21] and the amorphous/nanocrystalline alloys [22–26]. Magnetic multilayer systems provide a well defined structure which is ideally suited to study by microwave spectroscopy and SWR in particular. The treatment of mixed phase cluster type systems presents certain difficulties, particularly with respect to spin wave resonance, due to the randomness of the nucleation of crystallites. However, these may be overcome by making some simplifying assumptions in amorphous and nanocrystalline systems, due to the manner in which the nanocrystallites form, i.e. the crystallites grow in small grains of roughly equal size. When partially annealed, these materials consist of small ferromagnetic crystallites embedded in a ferromagnetic amorphous matrix [5–8]. This can also be readily applied to co-deposited alloys, where magnetic clusters are embedded in a non-magnetic matrix, such as Co–Cu, and GMR alloys [27].

In this paper we present the theory for ferromagnetic and spin wave multiphase magnetic materials. The theory is given for the general case of a single phase ferromagnet and then further developed for a double magnetic phase system, with some discussion as to the extension to an N phase system. This theory can be readily adopted for magnetic multilayer structures and amorphous/nanocrysalline mixed phase systems. In this regard we give the first description of amorphous/nanocrystalline materials within the FMR/SWR framework. This is particularly important since such systems have only quite recently been studied using ferromagnetic resonance, and in those cases where they have been studied, the analyses are given assuming a single magnetic phase [22–24]. In another publication we demonstrate the necessity of this approach in an experimental study of the crystallization of FeZrBCu by ferromagnetic resonance [28]. The theory here presented has much in common with analysis for FMR in magnetic multilayers by other authors [29–33], and indeed this theory gives analogous results when applied to layered structures, where we use a slightly different form of the boundary equation. The aims of this paper are to show the extension of this theory to the general case of a mixed phase ferromagnet, and in particular to apply it to amorphous and nanocrystalline mixed phase systems, where we outline some of the difficulties of the application of the theory. Of considerable importance are the changes that are undergone by such systems upon thermal annealing, where the samples gradually crystallize and the sample transforms from a reasonably homogeneous ferromagnetic amorphous phase through varying degrees of crystallinity, whereby ferromagnetic crystalline grains form in a remaining amorphous matrix. Both the crystalline grains and the amorphous phase change in magnetic properties during such

annealing processes [5–8, 34]. We emphasize the importance of grain size and shape effects, as well as grain boundary conditions.

2. Theory of ferromagnetic and spin wave resonance in single and multiphase magnetic materials

In this section we shall discuss the basic theory, firstly outlining that for a single phase ferromagnet, where we assume a homogeneous magnetization throughout the sample. Then we shall demonstrate the setting up of the boundary conditions, which is important for the spin wave resonance (SWR), and discuss the special case of ferromagnetic resonance (FMR). The theory will then be extended to the case of a multiphase ferromagnet, where we may assume that each phase has distinctly different magnetic properties, such as the magnetocrystalline anisotropy and magnetization. The application of this theory will be discussed for general mixed phase ferromagnets, where we discuss in detail the case of materials where grains of a ferromagnetic material are surrounded by another ferromagnetic material. This will apply to alloys of amorphous and nanocrystalline materials, such as the finemet type alloys etc, which have been thermally annealed [5].

2.1. Single phase materials

As this theory has already been dealt with by other authors, we shall only give a brief outline here, discussing the general theory of ferromagnetic and spin wave resonance and the application of boundary conditions to obtain the allowed spin wave wavevectors necessary for spin wave resonance.

2.1.1. General resonance equation. The ferromagnetic and spin wave resonance for a single phase material has been treated by several authors [16–20, 29–32] with certain variations. In the following we shall give a brief outline, where we will adopt a similar approach to that of [35], with some adjustments where convenient. We start from the equation of motion of the magnetization vector, which can be expressed in the form:

$$\frac{1}{\gamma}\frac{\partial \boldsymbol{M}}{\partial t} = \boldsymbol{M} \wedge \boldsymbol{H}_{eff}. \tag{1}$$

Equation (1) describes the motion or precession of the magnetization vector about that of the effective field, $\boldsymbol{H}_{eff}$. This effective field has various contributions depending on the sample (internal fields) and externally applied fields. The effective field can be written as:

$$\boldsymbol{H}_{eff} = \boldsymbol{H}_0 + \boldsymbol{h} + \boldsymbol{H}_K + \boldsymbol{H}_{ex} - \boldsymbol{H}_{dem} - \boldsymbol{H}_D. \tag{2}$$

$\boldsymbol{H}_0$ is the static (externally) applied field, $\boldsymbol{h}$ the microwave (rf) field, $\boldsymbol{H}_K$ represents the anisotropy field, $\boldsymbol{H}_{ex}$ the exchange field, $\boldsymbol{H}_{dem}$ the demagnetizing field resulting from sample shape and $\boldsymbol{H}_D$ is the damping field arising from relaxation effects. We can rewrite equation (1) in the form:

$$\frac{1}{\gamma}\frac{\partial \boldsymbol{M}}{\partial t} = \boldsymbol{\tau} + \boldsymbol{M} \wedge \boldsymbol{H}_{ex} - \boldsymbol{R} \tag{3}$$

where $\boldsymbol{M}$ is the magnetization vector, γ the magnetogyric ratio, $\boldsymbol{\tau}$ the torque introduced by the various magnetic contributions to the effective field, $\boldsymbol{H}_{eff}$, (excluding the exchange contribution, which has been left out of the torque term for purposes of clarity). The second term represents the effect of the exchange field vector, $\boldsymbol{H}_{ex}$. We treat the torque and exchange expressions explicitly, to show the spin wave term separately. The final term in

equation (3), $\boldsymbol{R}$, represents the relaxation term or damping vector, which will be neglected here, as we are primarily concerned with the resonance field; this could be included for linewidth analysis, and would take the form of the Landau–Lifshitz or Gilbert parameters, see for example [36]. Torque is defined as: $\boldsymbol{r} \wedge \boldsymbol{F}$, the moment of the force, and can be given in vectorial form as:

$$\boldsymbol{\tau} = \boldsymbol{e}_\vartheta \frac{1}{\sin\vartheta}\frac{\partial E}{\partial \vartheta} - \boldsymbol{e}_\phi \frac{\partial E}{\partial \phi} \tag{4}$$

where we are using a spherical polar coordinate system, see figure 1, where $\boldsymbol{e}_\vartheta$ and $\boldsymbol{e}_\phi$ are the unit vector in the ϑ and ϕ directions, respectively. At equilibrium, i.e. in the off-resonance state, the first derivatives of the free energy with respect to the angles, ϑ and ϕ, will be zero [35]. In this manner we can obtain the equilibrium orientation, ϑ_0 and ϕ_0, of the static magnetization vector. The magnetization vector is composed of a static and a dynamic component; $\boldsymbol{M}(\boldsymbol{r}, t) = \boldsymbol{M}_0(\boldsymbol{r}) + \boldsymbol{m}(\boldsymbol{r}, t)$, with the condition $|M_0| \gg |m|$, where M_0 is the static (or dc) component and m the dynamic (or rf) component. At resonance, the magnetization vector will be in motion, where the excursions from the equilibrium position can be expressed as:

$$\delta\vartheta = \vartheta - \vartheta_0 \qquad \text{and} \qquad \delta\phi = \phi - \phi_0. \tag{5}$$

Now

$$\sin(\delta\vartheta) \approx \delta\vartheta = \frac{m_\vartheta}{M_0} \qquad \text{and} \qquad \sin(\delta\phi) \approx \delta\phi = \frac{m_\phi}{M_0 \sin\vartheta}. \tag{6}$$

See figure 1 for explanation of the symbols. This gives the torque at resonance as:

$$\boldsymbol{\tau} = \left\{ \hat{\boldsymbol{e}}_\vartheta \frac{1}{\sin\vartheta}\frac{\partial^2 E}{\partial\phi\partial\vartheta} - \hat{\boldsymbol{e}}_\phi \frac{\partial^2 E}{\partial\vartheta^2} \right\} \frac{m_\vartheta}{M_0} + \left\{ \hat{\boldsymbol{e}}_\vartheta \frac{1}{\sin\vartheta}\frac{\partial^2 E}{\partial\vartheta^2} - \hat{\boldsymbol{e}}_\phi \frac{\partial^2 E}{\partial\vartheta\,\partial\phi} \right\} \frac{m_\phi}{M_0 \sin\vartheta}. \tag{7}$$

The exchange field, for bulk spins, is given by:

$$\boldsymbol{H}_{ex} = \frac{2A}{M_0^2}\nabla^2 \boldsymbol{m} \tag{8}$$

where A is the exchange stiffness constant (ergs cm^{-1}). From equations (3), (7) and (8), we can obtain the general resonance equation as:

$$\left(\frac{\omega}{\gamma}\right)^2 = \left(\frac{2A}{M_0}k^2\right)^2 + \left\{ \frac{1}{M_0 \sin^2\vartheta}\frac{\partial^2 E}{\partial\phi^2} + \frac{1}{M_0}\frac{\partial^2 E}{\partial\vartheta^2} \right\} \frac{2A}{M_0}k^2 + \frac{1}{M_0^2 \sin^2\vartheta}\left\{ \frac{\partial^2 E}{\partial\phi^2}\frac{\partial^2 E}{\partial\vartheta^2} - \left(\frac{\partial^2 E}{\partial\vartheta\,\partial\phi}\right)^2 \right\}. \tag{9}$$

This gives the most general form of the resonance equation for both spin wave resonance and ferromagnetic resonance, where it will be clearly noted that in the case of zero wavevector ($k = 0$), one obtains the uniform precession mode (i.e. the FMR limit), and equation (9) reduces to the well known Smit–Beljers equation [37]. For the case of spin waves in a confined magnetic system, such as a thin film in the perpendicular orientation or magnetic clusters, we must consider the boundary conditions to find the allowed spin wave wavevectors, k.

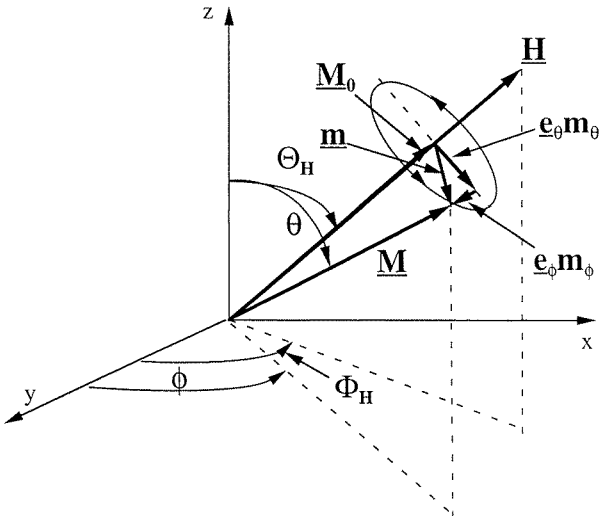

Figure 1. Spherical polar coordinate system. This shows the various components of the magnetization vector.

2.1.2. Boundary conditions. In any system where there is a magnetic discontinuity, the spins at a surface or interface will experience a different exchange field than those spins in the bulk of a ferromagnet due to the change of symmetry. Therefore we must take this into account in the equation of motion. This is given by the Rado–Weertman equation [38]:

$$\boldsymbol{M} \wedge \left(\frac{2A}{M_0}\right) \partial_n \boldsymbol{M} + \boldsymbol{\tau}_{surf} = 0 \tag{10}$$

where ∂_n denotes the outward normal derivative, i.e. the derivative in the direction perpendicular to the interface or boundary, and $\boldsymbol{\tau}_{surf}$ represents the surface or interface torque, where the surface torque is given by [35]:

$$\boldsymbol{\tau}_{surf} = \left\{ \boldsymbol{e}_\vartheta \frac{1}{\sin\vartheta} \frac{\partial^2 E_s}{\partial \vartheta^2} - \boldsymbol{e}_\phi \frac{\partial E_s}{\partial \vartheta \, \partial \phi} \right\} \frac{m_\phi}{M_0 \sin\vartheta} + \left\{ \boldsymbol{e}_\vartheta \frac{1}{\sin\vartheta} \frac{\partial^2 E_s}{\partial \phi \partial \vartheta} - \boldsymbol{e}_\vartheta \frac{\cos\vartheta}{\sin^2\vartheta} \frac{\partial E_s}{\partial \phi} - \boldsymbol{e}_\phi \frac{\partial^2 E_s}{\partial \vartheta^2} \right\} \frac{m_\vartheta}{M_0} \tag{11}$$

E_s represents the surface free energy density. The usual form of the surface energy is:

$$E_s = K_s \sin^2\vartheta \cos^2\phi \tag{12}$$

where K_s is the surface anisotropy.

Making the necessary derivatives of $m_{\vartheta,\phi}$ and the relevant substitutions, we can obtain the conditions for the allowed values of the spin wave wavevectors [32, 35]:

$$\frac{k(p_1+p_2)}{(p_1p_2-k^2)} = \tan(kL) \qquad \text{and} \qquad \frac{k(q_1+q_2)}{(q_1q_2-k^2)} = \tan(kL) \tag{13}$$

for volume or bulk modes, while for surface modes we have:

$$\frac{\mu(p_1+p_2)}{(p_1p_2-\mu^2)} = \tanh(\mu L) \qquad \text{and} \qquad \frac{\mu(q_1+q_2)}{(q_1q_2-\mu^2)} = \tan(\mu L). \tag{14}$$

In the perpendicular configuration, $\phi = 0$, it can be shown that $q_1 = p_1$ and $q_2 = p_2$. The subscripts refer to interfaces 1 and 2, for the general case where the two interfaces are non-symmetric. In this case the surface localized spin wave wavevectors are μ, where we write $k = \mathrm{i}\mu$. These will have a decaying nature.

2.2. Multiphase materials

2.2.1. General resonance equation. For the case of multiphase materials, by which we mean a material which contains more than one distinct magnetic phase, the situation is somewhat more complex. However, we can extend the theory used for the single phase ferromagnets to the case of multiphase samples. Such multiphase materials could be for example magnetic multilayer systems or alloys with a mixture of more than one magnetic phase, as is the case for amorphous and nanocrystalline materials. In this case we must set up the equation of motion for the magnetization vector for each individual magnetic phase. The exchange interaction between magnetic phases will be introduced into the free energy of the system as a whole, and the effect on any spin waves set up in any confined magnetic phase(s) will be manifest as a shift in the spin wave wavevector caused by the effect of the mutual exchange interaction at the boundaries. The equation of motion, then, for a phase A will be given as:

$$\frac{1}{\gamma_A}\frac{\partial \boldsymbol{M}_A}{\partial t} = \boldsymbol{\tau}_A + \boldsymbol{M}_A \wedge \boldsymbol{H}_{ex,A} - \boldsymbol{R}_A \tag{15}$$

which is just as given in the case of the single phase, equation (3). In this case, however, the torque expression will differ from the single phase case in that it will contain additional terms due to interactions with other magnetic phases. To illustrate this we shall take the example of a material with two magnetic phases. The equation of motion for this second phase, say B, will simply be given as in equation (15) where the A subscript will be replaced by B. The torque expression at resonance will now read:

$$\begin{aligned}\boldsymbol{\tau}_A = {} & \left\{\boldsymbol{e}_\vartheta \frac{1}{\sin\vartheta_A}\frac{\partial^2 E}{\partial\phi_A\partial\vartheta_A} - \boldsymbol{e}_\phi \frac{\partial^2 E}{\partial\vartheta_A^2}\right\}\frac{m_{\vartheta A}}{M_{0A}} + \left\{\boldsymbol{e}_\vartheta \frac{1}{\sin\vartheta_A}\frac{\partial^2 E}{\partial\vartheta_A^2} - \boldsymbol{e}_\phi \frac{\partial^2 E}{\partial\vartheta_A\partial\phi_A}\right\}\frac{m_{\phi A}}{M_{0A}\sin\vartheta_A} \\ & + \left\{\boldsymbol{e}_\vartheta \frac{1}{\sin\vartheta_A}\frac{\partial^2 E}{\partial\vartheta_B\partial\phi_A} - \boldsymbol{e}_\phi \frac{\partial^2 E}{\partial\vartheta_B\partial\vartheta_A}\right\}\frac{m_{\vartheta B}}{M_{0B}} \\ & + \left\{\boldsymbol{e}_\vartheta \frac{1}{\sin\vartheta_A}\frac{\partial^2 E}{\partial\phi_B\partial\phi_A} - \boldsymbol{e}_\phi \frac{\partial^2 E}{\partial\phi_B\partial\vartheta_A}\right\}\frac{m_{\phi B}}{M_{0B}\sin\vartheta_B}.\end{aligned} \tag{16}$$

(Compare equation (7).) The corresponding torque expression for phase B will be given by interchanging the A and B subscripts. For more phases we need to add further terms with the appropriate form in brackets, as given above for $m_{\theta B}$ and $m_{\phi B}$. Following the manipulations as given for a single phase, we can obtain the equations of motion in component form (these are given in appendix A). Solving in the usual manner, we obtain the following matrix [32]:

$$\begin{pmatrix} (\mathrm{i}\Omega_A - R_A) & -(P_A + D_A k_A^2) & -R_{BA} & -P_{BA} \\ (Q_A + D_A k_A^2) & (\mathrm{i}\Omega_A + R_A) & Q_{BA} & R'_{BA} \\ -R_{AB} & -P_{AB} & (\mathrm{i}\Omega_B - R_B) & -(P_B + D_B k_B^2) \\ Q_{AB} & R'_{AB} & (Q_B + D_B k_B^2) & (\mathrm{i}\Omega_B + R_B) \end{pmatrix} \begin{pmatrix} m_{\vartheta A} \\ m_{\phi A} \\ m_{\vartheta B} \\ m_{\phi B} \end{pmatrix} = 0 \tag{17}$$

where the substitutions for P_A, Q_A, etc are listed in appendix B. For non-trivial solutions the determinant goes to zero, from which we obtain the general resonance equation:

$$\begin{aligned}\{(\mathrm{i}\Omega_A - R_A)(\mathrm{i}\Omega_A + R_A) + (P_A + D_A k_A^2)(Q_A + D_A k_A^2)\}\{(\mathrm{i}\Omega_B - R_B)(\mathrm{i}\Omega_B + R_B) \\ +(P_B + D_B k_B^2)(Q_B + D_B k_B^2)\} - \{(\mathrm{i}\Omega_A - R_A)Q_{BA} + (Q_A + D_A k_A^2)R_{BA}\} \\ \times\{(\mathrm{i}\Omega_B + R_B)P_{AB} - (P_B + D_B k_B^2)R'_{AB}\} - \{(\mathrm{i}\Omega_A - R_A)R'_{BA} \\ +(Q_A + D_A k_A^2)P_{BA}\}\{(Q_B + D_B k_B^2)P_{AB} + (\mathrm{i}\Omega_B - R_B)R'_{AB}\} \\ -\{(P_A + D_A k_A^2)Q_{BA} - (\mathrm{i}\Omega_A + R_A)R_{BA}\}\{(P_B + D_B k_B^2)Q_{AB} \\ -(\mathrm{i}\Omega_B + R_B)R_{AB}\} - \{(P_A + D_A k_A^2)R'_{BA} - (\mathrm{i}\Omega_A + R_A)P_{BA}\} \\ \times\{(Q_B + D_B k_B^2)R_{AB} + (\mathrm{i}\Omega_B - R_B)Q_{AB}\} - \{R_{BA}R'_{BA} - P_{BA}Q_{BA}\} \\ \times\{P_{AB}Q_{AB} - R_{AB}R'_{AB}\} = 0. \qquad (18)\end{aligned}$$

It will be readily seen that for the case of non-interacting magnetic phases, e.g. for decoupled magnetic layers, equation (18) will reduce to two uncoupled resonance equations of the form of equation (9). This method can be extended to a system of N phases, where the solution will be obtained from a $2N \times 2N$ matrix.

2.2.2. Boundary conditions. In addition to accounting for the energy of interaction between the various magnetic phases in a sample, we must also take into account the effect that the magnetic phases will have on each other at their interfaces. This will affect the pinning conditions for the allowed spin wave modes, where we have to introduce further interaction terms into the boundary equations. This will produce a shift in the resonance field, due to the effect of the changed boundary conditions, with respect to the case of an isolated single phase sample. The number of boundary equations will depend on the sample, i.e. the number of phases and interfaces. In the case of a magnetic multilayer system, this will be very systematic, and well defined in a one-dimensional manner [32, 39–41]. For the case of a mixed phase material, as for nanocrystalline systems, we must use a slightly different approach. This will greatly depend on the nature of the sample itself.

In any case we must take the boundary conditions for each phase which can support spin wave modes, individually. As stated, this will depend on the conditions surrounding that particular phase. In order to continue we shall have to make some simplifying assumptions, which will be valid for certain types of sample. We will set up the general boundary equations, and later discuss the various physical restrictions which should be adopted in certain cases, giving some examples. In the case of nanocrystalline systems, it is commonly found that nanocrystals form in a surrounding ferromagnetic amorphous matrix, after annealing at an appropriate temperature for a certain time [5, 8]. For the finemets and other amorphous alloys the sizes of these nanocrystallites are of the order of 10–20 nm [5], a size which may physically support standing spin wave modes. The form of these spin waves will also depend on other factors, such as the exchange stiffness constant and magnetization. In certain cases, the amorphous phase may not be homogeneous, and there may be more than one distinct magnetic phase [42, 43]. Effects such as these can produce additional resonances in the SWR/FMR spectra, cause averaging effects in the resonance field (section 3.1) and may have significant effects on resonance linewidths.

For purposes of simplicity, we shall consider the case of a double magnetic phase, where one magnetic phase is surrounded by another. The resulting spectra will be an average over the whole sample, where we assume that the grains are approximately of the same size. The physical spectra from such a sample will show a broadening of the resonance peaks,

which is related to the spread of grain size from the average [25]; this will also be true for any variations of the magnetization etc. For the present we shall assume that the transverse wavevector is zero, whereas in reality this may not be the case; this will be further discussed later (section 3.3). The transverse direction will be defined as the directions perpendicular to the applied magnetic field.

We consider the case where a ferromagnetic material A is surrounded by a ferromagnetic material B. In this situation we shall consider the average grain, with two boundaries separated by a distance L, where, as the grain is completely enclosed in material B, the pinning conditions at the two interfaces can be assumed to be identical. The boundary equations can now be written in the form:

$$\boldsymbol{M}_A \wedge \left(\frac{2A_A}{M_{0A}^2}\right)\partial_n \boldsymbol{M}_A - \boldsymbol{M}_A \wedge \left(\frac{2A_{AB}}{M_{0A}M_{0B}}\right)\partial \boldsymbol{M}_B + \boldsymbol{\tau}_{int.AB} = 0. \tag{19}$$

This has the same basic form as the Rado–Weertman boundary equation, see equation (10), where we have an additional term due to the magnetic exchange interaction between the magnetic phases A and B. This term has been defined such that the interaction between the magnetic phases is of the form of a stiffness constant, A. Subsequent treatment will be analogous to that for the single phase. For the case of magnetic multilayers it is, in general, necessary to set up the boundary conditions at each interface explicitly [32, 39–41]. The static components can be expressed as:

$$\begin{aligned}
&\left(\frac{2A_A}{M_{0A}}\right)(\partial_n M_{0A})_\vartheta - \left(\frac{2A_{AB}}{M_{0B}}\right)(\partial_n M_{0B})_\vartheta + \frac{\partial E_{int}}{\partial \vartheta_A} = 0 \\
&\left(\frac{2A_A}{M_{0A}}\right)(\partial_n M_{0A})_\phi - \left(\frac{2A_{AB}}{M_{0B}}\right)(\partial_n M_{0B})_\phi + \frac{1}{\sin\vartheta_A}\frac{\partial E_{int}}{\partial \vartheta_A} = 0
\end{aligned} \tag{20}$$

where E_{int} is the interfacial energy. While the components of the dynamic boundary conditions are:

$$\begin{aligned}
&\partial_n m_{\vartheta A} + \frac{A_{AB}}{A_A}\frac{M_{0A}}{M_{0B}}\partial_n m_{\vartheta B} + p m_{\vartheta A} + q m_{\vartheta B} + r m_{\phi A} + s m_{\phi B} = 0 \\
&\partial_n m_{\phi A} + \frac{A_{AB}}{A_A}\frac{M_{0A}}{M_{0B}}\partial_n m_{\phi A} + r m_{\vartheta A} + t m_{\vartheta B} + u m_{\phi A} + v m_{\phi B} = 0
\end{aligned} \tag{21}$$

where the substitutions for p, q, r, s, t, u and v are listed in appendix B. When we take the interface energy, which has the form:

$$E_{int} = K_{int}^{AB}\sin^2\vartheta_A\cos^2\phi_A \tag{22}$$

we see that the terms q, s, t and v will go to zero. Furthermore, due to geometric considerations r also goes to zero, greatly simplifying the boundary equations. In equation (22) K_{int}^{AB}, represents the interfacial anisotropy, which is given here in uniaxial form. Taking the appropriate derivatives and back substituting we obtain the pinning parameters:

$$\begin{aligned}
p &= \frac{K_{int}^{AB}}{A_A}(\cos^2\vartheta_A - \sin^2\vartheta_A)\cos^2\phi_A + \frac{A_{AB}}{A_A}\frac{\partial_n M_{0B}}{M_{0B}} - \frac{\partial_n M_{0A}}{M_{0A}} \\
u &= \frac{K_{int}^{AB}}{A_A}(\sin^2\phi_A - \sin^2\vartheta_A\cos^2\phi_A) + \frac{A_{AB}}{A_A}\frac{\partial_n M_{0B}}{M_{0B}} - \frac{\partial_n M_{0A}}{M_{0A}}.
\end{aligned} \tag{23}$$

In fact, it can be seen from this analysis that the boundary equations are very similar to that for a single phase [32, 35]. The are differences however, these being that the contributions to the pinning parameters here have additional terms relating to the coupling

between the magnetic phases. In the case where $M_{0A} = M_{0B}$, and $A_{AB} = A_A$, the sample effectively becomes magnetically continuous, with no effective boundary. In this situation the interface anisotropy constant K_{int}^{AB} will become zero, thus the pinning parameters will tend to zero and the boundary equations will naturally collapse.

In our case of the mixed phases, the pinning conditions will be symmetric, thus yielding the allowed spin wave wavevectors (cf equations (13) and (14)):

$$\frac{2k_A p}{p^2 - k_A^2} = \tan(k_A L) \qquad \text{and} \qquad \frac{2k_A u}{u^2 - k_A^2} = \tan(k_A L) \tag{24}$$

for bulk modes, and

$$\frac{2\mu_A p}{p^2 - \mu_A^2} = \tanh(\mu_A L) \qquad \text{and} \qquad \frac{2\mu_A u}{u^2 - \mu_A^2} = \tanh(\mu_A L) \tag{25}$$

for interface localized modes. L is the average grain size. As stated, this makes the assumption that k, the spin wave wavevector, perpendicular to the direction of the applied field is zero. In the case of the multilayer system, the form of the boundary equations will be as given above, with the further addition of the outer boundaries at the sample extremes. Also, the boundary equations may not be symmetric [32] and the equations giving the allowed wavevectors will be as in equations (13) and (14), using pinning parameters given in equation (23).

2.2.3. Free energy considerations. In order to use the resonance equations, we need to obtain the expression for the free energy of the whole system. Then we have to perform the relevant derivatives with respect to θ and ϕ, and substitute them into the resonance equation. For a system of N phases, we can represent the free energy of the whole sample as:

$$E = \sum_{n=1}^{N} \Big\{ V_n [-M_{0n} H [\sin\vartheta_n \sin\Theta_H \cos(\Phi_H - \phi_n) + \cos\vartheta_n \cos\Theta_H] \\ -2\pi M_{0n}^2 \sin^2\vartheta_n + E_K^n(\vartheta_n, \phi_n)] - \boldsymbol{M}_n \cdot \sum_m K_{nm} \boldsymbol{M}_m \Big\}. \tag{26}$$

V_n represents the relative quantities of each phase, and is dimensionless, where the following relation holds:

$$\sum_n V_n = 1. \tag{27}$$

So V_n for each phase will give the relative volume of that phase in the sample. The first summation, in equation (26), will be over the number of phases present. Angles with H subscripts represent the orientation of the applied field H, see figure 1. The first term in square brackets (in equation (26)) represents the Zeeman energy, the second term the demagnetizing energy for an isotropic sample, and the third term, $E_K^n(\vartheta_n, \phi_n)$, represents the magnetocrystalline anisotropy energy of each phase, where different anisotropies can be readily adopted, depending on the type of crystal [29, 30, 44]. The second summation over m, where $m \neq n$, will be over the magnetic interaction between neighbouring phases, which will depend greatly on the nature of the sample. In the case of a multilayer system, it will be over neighbouring or adjacent layers, while for a mixed phase sample would be over all phases that are strictly in 'magnetic contact', i.e. those magnetic phases which feel

the effect of the other magnetic phases. By way of illustration, it can be shown that the interaction energy between phases A and B, this has the form:

$$E_{AB} = -K_{AB}\boldsymbol{M}_A \cdot \boldsymbol{M}_B = -K_{AB}M_{0A}M_{0B}\{\sin\vartheta_A \sin\vartheta_B \cos(\phi_A - \phi_B) + \cos\vartheta_A \cos\vartheta_B\} \tag{28}$$

where

$$K_{AB} = \frac{J_{AB}}{|M_{0A}||M_{0B}|}.$$

K_{AB} will be a measure of the strength of the exchange interaction between the magnetic phases (and J_{AB} the exchange energy). For the case of ferromagnetic coupling K_{AB} will be positive, giving parallel alignment of M_A and M_B for an energy minimum. In the case of an intervening non-magnetic material, the coupling interaction could be negative, i.e. antiferromagnetic alignment, where an energy minimum is found when M_A and M_B are antiparallel; in this case K_{AB} will be negative. For the case of multilayers, an extra term of the form $-K'_{AB}(\boldsymbol{M}_A\boldsymbol{M}_B)^2$ may be introduced to account for biquadratic coupling [12], where M_A and M_B are aligned perpendicularly for an energy minimum.

3. Applications to specific multiphase ferromagnets

The case for magnetic multilayered structures has been quite extensively discussed by several authors. The results using the present method are in accord with those of other authors [16–21, 29–32]. The case for nanocrystalline materials, which constitute a more complicated magnetic multiphase system, has not received much attention with regard to ferromagnetic and spin wave resonance. This will be addressed in section 3.3, giving a detailed discussion of the effects of the nanocrystallized grains, where confinement effects inside the grains may give rise to spin wave modes, and how the surrounding phase will affect these resonances. We shall give the example of cubic grains as a simple case, applying the boundary conditions to give the allowed values of the k vectors of the standing spin wave modes. Then we shall discuss the modifications necessary when dealing with more realistic cases of different shaped grains. In the following section we show the analysis for the determination of the resonance field in the case of a general mixed phase ferromagnet, which applies to both magnetic multilayers and general random mixed phases.

3.1. Mixed double phase ferromagnet

We now consider the case of a two phase ferromagnet. The sample will be set in the x–y-plane, as illustrated in figure 2. We must now take the derivatives of the free energy with respect to the angles. The first derivatives of the free energy, as given in equation (26), with respect to the angles are set to zero, from which we obtain the equilibrium conditions, which, for phase A, will be

$$H\sin(\Phi_H - \phi_A) = H_{KA}\sin\phi_A\cos\phi_A - \frac{K_{AB}}{V_A}M_{0B}\sin(\phi_A - \phi_B). \tag{29}$$

It will be noted that we have taken the case for uniaxial magnetocrystalline anisotropy. That for B is simply found by swapping the A and B subscripts, where the anisotropy field, H_{KA}, is given by:

$$H_{KA} = \frac{2K_A^u}{M_{0A}}. \tag{30}$$

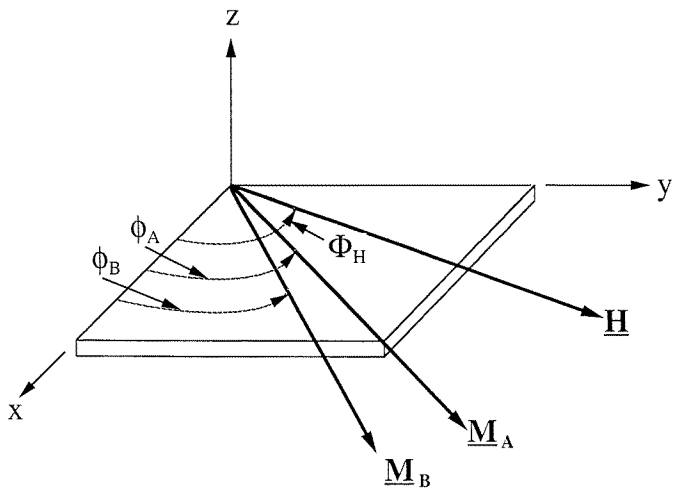

Figure 2. In-plane geometry and coordinate system for a two phase magnetic system.

The second derivatives of the free energy are given in appendix C. When we take account of the sample orientation, i.e. placing the sample in the x–y-plane, the cross derivative terms, i.e. those with respect to θ and ϕ (the R terms), go to zero. This greatly simplifies the resonance equation (18), which will now read:

$$\begin{aligned}\{-\Omega_A^2 + (P_A + D_A k_A^2)(Q_A + D_A k_A^2)\}\{-\Omega_B^2 + (P_B + D_B k_B^2)(Q_B + D_B k_B^2)\} \\ -\Omega_A\Omega_B\{P_{BA}Q_{AB} + P_{AB}Q_{BA}\} + P_{AB}P_{BA}(Q_A + D_A k_A^2)(Q_B + D_B k_B^2) \\ -Q_{AB}Q_{BA}(P_A + D_A k_A^2)(P_B + D_B k_B^2) + P_{AB}P_{BA}Q_{AB}Q_{BA} = 0. \qquad (31)\end{aligned}$$

Due to the form of the free energy and the resonance equation, it is convenient to redefine some of the parameters. This will not affect the physics of the resonance equation, and will aid the manipulation of the equation above. We will now write:

$$\Omega_N = \frac{\omega}{\gamma_N} M_{0N} \sin\vartheta_N. \qquad (32)$$

Other changes will be to the parameters P, Q and R, where the denominators will no longer have an M_{0N} term. With a little manipulation we can gather the terms which involve the exchange interaction constant K_{AB}, where $P'_A = P_A - P_{AB}$ etc. Also we note that $P_{AB} = P_{BA}$ and $Q_{AB} = Q_{BA} = K_{AB}M_{0A}M_{0B}$ and in the present geometry we can put $\theta_A = \theta_B = \pi/2$, $P_{AB} = Q_{AB}\cos(\phi_A - \phi_B)$. Now the resonance equation can now be written:

$$\begin{aligned}\{-\Omega_A^2 + (P_A + D_A k_A^2)(Q_A + D_A k_A^2)\}\{-\Omega_B^2 + (P_B + D_B k_B^2)(Q_B + D_B k_B^2)\} + K_{AB}M_{0A}M_{0B} \\ \times\{[(Q'_B + D_B k_B^2) + (P'_B + D_B k_B^2)][(P'_A + D_A k_A^2)(Q'_A + D_A k_A^2) - \Omega_A^2] \\ +[(Q'_A + D_A k_A^2) + (P'_A + D_A k_A^2)][(P'_B + D_B k_B^2)(Q'_B + D_B k_B^2) - \Omega_B^2]\} \\ +K_{AB}^2 M_{0A}^2 M_{0B}^2\{[(P'_A + D_A k_A^2) + (P'_B + D_B k_B^2)] \\ \times[(Q'_A + D_A k_A^2) + (Q'_B + D_B k_B^2)] - (\Omega_A + \Omega_B)^2\} = 0. \qquad (33)\end{aligned}$$

In the case of very strong coupling, where $K_{AB} \gg 1$, the final term involving K_{AB}^2 will dominate. In this situation we would expect $\phi_A = \phi_B = \phi$. Therefore the resonance equation will simplify to:

$$(\Omega_A + \Omega_B)^2 = [(P'_A + D_A k_A^2) + (P'_B + D_B k_B^2)][(Q'_A + D_A k_A^2) + (Q'_B + D_B k_B^2)]. \qquad (34)$$

This equation will be valid for the case of a magnetic bilayer and a material with two strongly coupled magnetic phases. Equation (34) is valid for the general case of spin wave resonance in both phases A and B. For the magnetic bilayer situation, we can now adopt the relevant boundary conditions to obtain the k-values. The case for a mixed phase is more problematic in that we need to define the region in which the spin wave are excited, in a rigid manner. That is, we must define the size and properties, as well as the boundaries for such a phase. Should we only consider the case of ferromagnetic resonance, equation (34) would reduce to that obtained by Layadi and Artman [31]. Substituting for the various parameters (see appendix B, equation (B1)), we find that the resonance equation yields:

$$\left(\frac{\omega}{\gamma_{eff}}\right)^2 = \{H\cos(\Phi_H-\phi)+H_K^{eff}(\sin^2\phi-\cos^2\phi)+D'_Ak_A^2+D'_Bk_B^2\}\{H\cos(\Phi_H-\phi) +4\pi M_0^{eff}-H_K^{eff}\cos^2\phi+D'_Ak_A^2+D'_Bk_B^2\} \tag{35}$$

with equilibrium condition:

$$H\sin(\Phi_H-\phi)=H_K^{eff}\sin\phi\cos\phi \tag{36}$$

where

$$H_K^{eff}=\frac{V_AH_{KA}M_{0A}+V_BH_{KB}M_{0B}}{V_AM_{0A}+V_BM_{0B}} \tag{37}$$

is the effective anisotropy field,

$$M_0^{eff}=\frac{V_AM_{0A}^2+V_BM_{0B}^2}{V_AM_{0A}+V_BM_{0B}} \tag{38}$$

is the effective magnetization,

$$\gamma_{eff}=\frac{V_AM_{0A}+V_BM_{0B}}{V_AM_{0A}/\gamma_A+V_BM_{0B}/\gamma_B} \tag{39}$$

is the effective magnetogyric ratio, and

$$D'_A=\frac{V_AM_{0A}D_A}{V_AM_{0A}+V_BM_{0B}}\text{etc} \tag{40}$$

is the redefined spin wave constant. Therefore, we can see that equation (35) is of the form of a resonance equation for a single phase, with parameters as given in equations (37)–(40), in other words, is like an average over the phases present. It should be noted that we must treat the spin wave resonance case in each phase separately. Although the spin wave term is present in equations (34) and (35) for both phases, we must put $k_B = 0$ in magnetic phase A and $k_A = 0$ in magnetic phase B, i.e. the spin wave wavevector in phase A for phase B is zero, and vice versa. As stated previously, for a zero coupling case the resonance equation (33) reduces to that for isolated single phase resonances.

The variation of the effective magnetization, from equation (38), is illustrated as a function of the content of phase A in figure 3. The value of M_{0A} is kept constant at 1000 G, where the figure is given for selected values of M_{0B}. In figure 4, we illustrate the effect of the magnetization values on the resonance field, in which the values for the anisotropy fields are 20 and 10 G, for phases A and B, respectively. The value of the magnetization for phase A was kept at 1000 G while various values are shown for that of phase B. In figure 5, the values for the magnetization of phases A and B are 1000 G and 750 G, respectively. The value of H_{KB} is kept at zero, and we show the variation of the resonance field as a function of the phase A content for values of H_{KA} of 200, 0 and -200 G. We see that the effect of the uniaxial anisotropy field is fairly insignificant, this

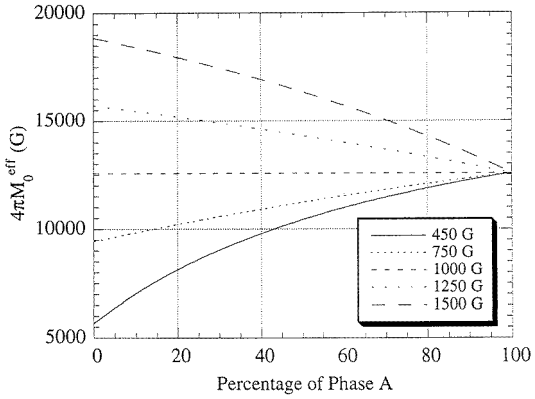

Figure 3. Variation of $4\pi M_0^{eff}$ in the strong ferromagnetic coupling limit, using equation (38), where M_{0A} is kept at 1000 G, and M_{0B} is given selected values as indicated.

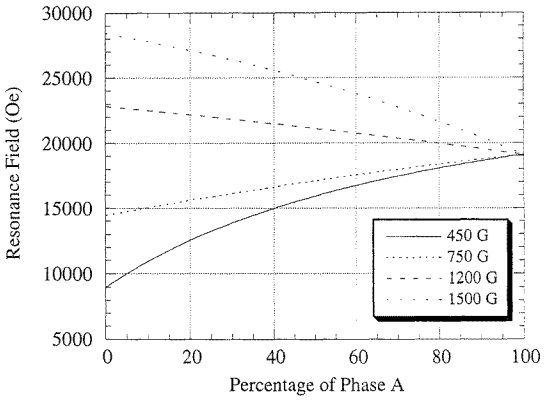

Figure 4. Effect of change of magnetization on the resonance field. Here we use equation (35), with $M_{0A} = 1000$ G, for selected values of M_{0B}, as indicated.

is especially so in the case of amorphous/nanocrystalline materials, where the anisotropy is generally small. We use equation (35) for these simulations. The simulations are all in the FMR limit with strong ferromagnetic coupling, where the magnetic field applied along the $\phi = 0$ direction.

For the case of weak to zero exchange coupling, we expect two ferromagnetic resonance peaks, which would correspond to those of the isolated resonance fields (these will be given by the extreme values of the resonance field in figure 4). These result from equation (33), which is fourth order in H, where two solutions are physically meaningful, see also [31] and [33]. As the exchange coupling interaction increases in strength, the two resonances will be expected to move to a common point, depending on their relative concentrations, until they are degenerate at the full ferromagnetic coupling limit.

In a separate publication [28] we give a detailed experimental study of the system $Fe_{87}Zr_6B_6Cu$ by ferromagnetic resonance. Here the FMR spectra have been taken at different stages in the crystallization process, which gives rise to various magnetic phases. These magnetic phases interact magnetically and are in good agreement with the theory discussed in the present article.

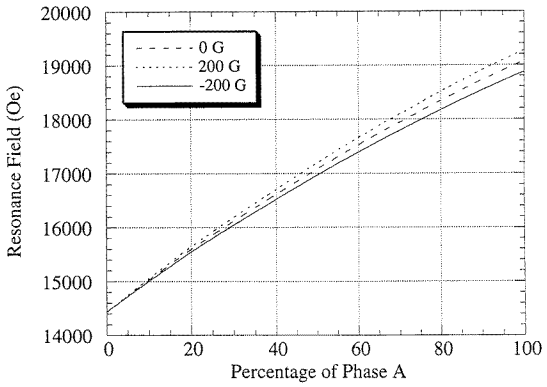

Figure 5. Effect of change of anisotropy field on the resonance field. Using equation (35), with $M_{0A} = 1000$ G, $M_{0B} = 750$ G and $H_{KB} = 0$ G. Values of H are indicated.

For the inclusion of spin wave resonance, it is necessary to define the region in which the spin wave modes are excited. The exchange coupling will affect the pinning parameters, as described in section 2.2.2, thus causing a change in the spin wave wavevectors, producing a corresponding shift in the resonance field. This has been discussed by several authors for the case of magnetic multilayers [16–19, 32, 45, 46] using various approaches. The case for amorphous and nanocrystalline materials is discussed in section 3.3.

3.2. Magnetic multilayers

The case for a magnetic multilayered structure can be treated in a systematic manner by applying the boundary conditions at the interfaces of each magnetic layer. In this manner, we can obtain the allowed conditions for spin wave resonance modes in each of the magnetic layers as a function of the pinning parameters at each interface. It will be noted that while the exterior boundaries will have pinning parameters analogous to those of a single magnetic layer, the interior magnetic boundaries will have pinning parameters which contain an additional contribution which will be dependent on the size and strength of the interlayer magnetic coupling, as discussed previously. Such an approach can be shown to give results which are consistent with the findings of other authors [16–18, 45, 46].

3.3. Amorphous and nanocrystalline mixed phase systems

In the as-cast state, some amorphous alloys tend to be inhomogeneous, and their resulting magnetization can therefore be expected to be inhomogeneous. This is certainly the case for FeZrCuB and FeZr amorphous alloys grown by melt spinning [22–24, 28, 42, 43]. It may therefore be contended that these materials should be, strictly speaking, treated in the multiphase manner discussed above; this will be particularly true when such materials have been partially annealed, where two clear ferromagnetic phases are present. In the case of very strong coupling between phases it has been shown, section 3.1, that one can adopt a ‘single phase’ stance for the case of ferromagnetic resonance (where the wavevectors will be zero), though it must be remembered that this is essentially an averaging of the magnetism of the phases present, in which case we need to use the parameters (36)–(39). For the case of spin wave resonance, the situation will be a little more complex as we must consider the possibility of further resonances in the spectra, due to a confinement effect arising from the boundary or interfacial conditions, where we additionally need to use the spin wave parameters, equation (40).

In the case of partially annealed materials, a nanocrystallization takes place in which one phase (i.e. that which crystallizes) will co-exist with the ferromagnetic amorphous phase, where in general they have a distinct magnetic behaviour. When this phase presents two boundaries with the other phase, that is a confined magnetic phase, in the direction of the applied field, a standing spin wave resonance may be excited. The nature of this spin wave resonance will depend on the properties of the two magnetic phases, the interface which separates them (i.e. the confinement length) and the orientation of the applied magnetic field. We may consider the case that, for example, should the spins at the interior of the enclosed phase have a greater freedom than those at the interface, then a bulk type spin wave will result, whereas if the interface spins have a greater freedom than those of the bulk spins then an interface localized spin wave mode will be expected. This will depend greatly on the exchange stiffness constants of the two materials as well as the interfacial anisotropy.

With further annealing the nature of the samples will change and it would be expected that the dominant magnetic properties will go through an effective phase transition, from that of the amorphous phase to that of the complete polycrystalline phase. This is clearly observed in the case of finemets [25]. In certain materials other phases may crystallize and new resonances may be expected to result; this is observed in FeZrCuB [28]. We can further expect the magnetic properties of the amorphous phase(s) to alter with annealing, as magnetic atoms are 'removed' to form the crystalline phase, and therefore the effective amount of magnetic ions in the amorphous phase will be reduced [43, 48]. Such processes, in materials like the finemets, cause an increase in the inhomogeneity of the amorphous phase, which may also give rise to further resonances [28]. In these types of material we are justified in using the strong coupling limit, as there is generally no intervening non-magnetic phase, or if there are any, they are in a small enough quantity not to affect the strong ferromagnetic interaction between magnetic phases. It may, however, be argued that as the amorphous phase becomes depleted of magnetic ions (which inevitably occurs in the annealing process), generally Fe, the coupling will reduce in strength. This is taken into account in the exchange interaction, equation (28). In this case we would have recourse to the most general form of the resonance equation (33).

Another consideration will be the assumption made about the zero transverse spin wave wavevector. For small clusters of ferromagnetic materials, we should account for the non-zero transversal wavevector, arising from the size of the grains. This may be expected to have an effect on the field position of the spin wave resonances which may arise from these phases. This will necessitate the consideration of the boundary conditions over the entire surface of the ferromagnetic grains.

We shall consider the case of cubic crystallites of a magnetic phase, with magnetization M_A, embedded in another magnetic phase, of magnetization M_B. This is a crude approximation of the situation described above, where magnetic crystallites are embedded in a surrounding amorphous magnetic matrix. Figure 6 shows an illustration of this situation, where the average crystallite has a length d in the directions x, y and z. We shall consider the applied external field as along the y direction and we can assume that the transversal components of the spin wave wavevectors are zero. The boundary equations at the interfaces at $y = 0$ and $y = d$ will be symmetric and of the form written in equation (19), with static and dynamic components given by equations (20) and (21). Thus we can write the boundary equations as:

$$\text{at } y = 0: \qquad \alpha_A P^{int} + \beta_B k_A = 0 \tag{41}$$

$$\text{and at } y = d: \qquad \alpha_A\{P^{int}\cos k_A d + k_A \sin k_A d\} + \beta_A\{P^{int}\sin k_A d - k_A \cos k_A d\} = 0 \tag{42}$$

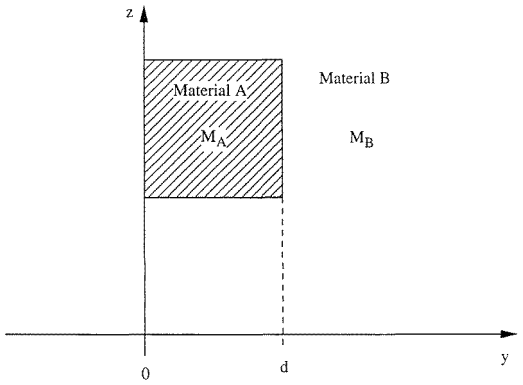

Figure 6. Magnetic grain, of length d in the y-direction, with magnetization M_A, embedded in the matrix of a magnetic material with magnetization M_B.

where the interfacial pinning parameter will be given by:

$$P^{int} = -d\frac{K_{AB}^{int}}{A_A} + \frac{A_{AB}}{A_A}\frac{\partial_n M_B}{M_{0B}} - \frac{\partial_n M_A}{M_{0A}}. \tag{43}$$

(This will be identical to the internal pinning parameter for magnetic multilayers.) Following the usual manipulations we obtain the equation of allowed k vectors in the magnetic particle A as:

$$\tan k_A d = \frac{2k_A P^{int}}{[(P^{int})^2 - k_A^2]}. \tag{44}$$

This gives the expected form, which is analogous to that for a single 'layer', which in effect is what we have described. The difference in this case from that of the single isolated magnetic layer, is that there will be a term in the expression for the pinning parameter, which depends on the magnetic coupling between the magnetic particle and the surrounding magnetic phase. This is as expected in this situation, since the individual magnetic particle will behave as a single body which can support spin wave resonance modes. So for the case of very strong pinning, we can obtain Kittel type modes inside the magnetic grains. The effect of grain size on the field positions of spin wave resonance modes is illustrated in figure 7. Here we show a sample where the grains have a magnetization of 750 G (surrounded by a material with a magnetization 1000 G), uniaxial anisotropy field of 20 G and $g = 2$. The first five resonance modes are illustrated where (a) $A = 1 \times 10^{-7}$ erg cm^{-1} and (b) $A = 6 \times 10^{-7}$ erg cm^{-1}; note the scales on the 'resonance field' axes. We see that for small grain sizes the SWR modes are well separated and gradually converge to the uniform mode position ($k = 0$) as the grain size increases. For small values of the exchange stiffness constant, A, the various spin wave modes will not be distinguishable since the linewidths of the modes will produce an overlap between adjacent spin wave modes, note scale in figure 7(a). In this example we use the strong coupling limit. Although we have assumed that the pinning is very strong at the grain boundaries in this example, we would expect a similar response for other pinning strengths, where this would introduce a shift in the resonance field positions, from those shown in figure 7, due to the different k-values. For the mixed phases presented by amorphous and nanocrystalline systems, we are justified in using the strong FM coupling limit, as the two ferromagnetic phases are always in close contact. Therefore, as the crystalline phase grows (with annealing), the amorphous phase

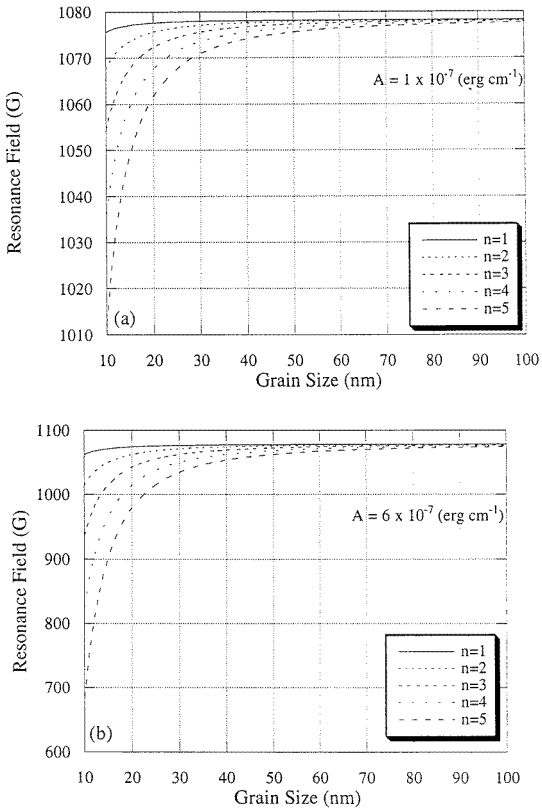

Figure 7. Effect of grain size on the spin wave resonance field for the first five spin wave modes. The grains are assumed to have strong pinning at the interfaces of the grains. These are shown for exchange stiffness constants of (a) $A = 1 \times 10^{-7}$ erg cm^{-1} and (b) 6×10^{-7} erg cm^{-1}.

loses magnetic atoms (which form the crystalline phase) and hence becomes magnetically weaker. From equation (33), we expect that the resonance will approach the FMR (or single phase) position for the crystalline phase. It is important to remember that as the crystallites grow there may be an intergrain magnetic interaction, which would also tend to the FMR mode as the intergrain separation reduces and the crystallites coalesce.

To model the change of field position of the FMR absorption peak is rather complex, in a realistic situation, as there is more than one parameter that changes as the sample crystallizes. If we assume a simple situation where one phase grows at the expense of the other in a two phase system, then we must not only account for the change of the relative volumes of the two phases, but also the changes in the magnetizations of the two phases and the effect that this will have on the strength of the coupling constant. This is clearly very complex, and in any analysis of experimental data of this nature must be taken into account at each stage in the crystallization process [28].

Should there be an interaction between the magnetic particles, this can also be taken into account by adding another magnetic interaction term into the boundary equation for the inter-particle magnetic coupling, which can be of variable strength. This should be included in the equation for the resonance field, equation (33). In such a case we would have to consider the average separation between crystallites. Furthermore, this analysis would be

the same for a material which has a magnetic phase dispersed in a non-magnetic matrix, such as for example, Co–Cu co-deposited alloys. The spin wave modes would be described by equation (44) where the interaction between magnetic particles is accounted for in the pinning parameter.

So far we have only considered the situation where $k = k_y$, i.e where the transversal components of the wavevectors are zero. If the magnetic particles were of an arbitrary shape this assumption would no longer hold, as standing spin wave modes could be set up in the x- and z-directions. In this case we must consider the wavevector in three dimensions, where we write:

$$k = \{\langle k_x \rangle^2 + \langle k_y \rangle^2 + \langle k_z \rangle^2\}^{1/2} \tag{45}$$

where $\langle k_x \rangle$ represents the average value of k_x, the x-direction component of the wavevector. So to evaluate the average components of the wavevector we have to consider each component separately. This leads to a simple averaging over the entire grain in each of the three coordinate directions, such that:

$$\langle k_x \rangle = \frac{1}{m}\left\{ \sum_{m'} k_{m'}^2 \right\}^{1/2} \tag{46}$$

$$\langle k_y \rangle = \frac{1}{n}\left\{ \sum_{n'} k_{n'}^2 \right\}^{1/2} \tag{47}$$

$$\langle k_z \rangle = \frac{1}{p}\left\{ \sum_{p'} k_{p'}^2 \right\}^{1/2} \tag{48}$$

where m, n and p refer to the number of sites in each of the x-, y- and z-directions, respectively, and m', n' and p' refer to site labels. Such an averaging over the wavevectors can be expected to cause a linewidth broadening of the resonance absorption lines. This contribution to the linewidth can be expressed as:

$$\Delta H_k = \frac{4A}{M_0} k \Delta k \tag{49}$$

where Δk represents the spread of values of k. For any regular shaped grains, such as spherical or cubic, an averaging of the wavevectors will not be expected to give a shift from the k_y-value (for the applied field along the y-direction), as $\langle k_x \rangle \sim 0$ and $\langle k_z \rangle \sim 0$, therefore $k \approx k_y$. There would, however, be a broadening associated with such a resonance, which will depend on the grain size. Irregular shaped grains may be expected to give a shift in the field position of resonances, as the transversal components of k will no longer average to zero. This would be strongly dependent on the shape and asymmetry of the grains.

Another important consideration in these types of sample is the effect that a spread of grain size will have on the linewidth. For the case of strong pinning, we expect an additional contribution to the linewidth of the form:

$$\Delta H_d = \frac{4A}{M_0} \frac{n^2 \pi^2}{d^3} \Delta d \tag{50}$$

where Δd represents the spread of grain size and n is the modal number. This broadening is linear with the spread of grain size, where the gradient is dependent on the material constants of the sample, and falls as $1/d^3$ with increase of grain size for a constant value of Δd. So for a sample of $M_0 = 750$ G, $A = 1 \times 10^{-7}$ erg cm^{-1}, with grain size, $d = 20$ nm and spread of grain size, $\Delta d = 2$ nm, we expect a broadening of about 132 G in the

linewidth of the $n = 1$ spin wave resonance mode. This would also be valid for the case of magnetic multilayers, where a spread in magnetic layer thickness will induce a linewidth broadening, where we should replace d with the layer thickness L, where ΔL would be the rms roughness of both interfaces. This shows that interfacial roughness is an important factor in magnetic thin films and magnetic multilayers, where we may also expect a spread in exchange interaction across the multilayer, which in turn will cause further broadening effects.

4. Conclusions

The theory of ferromagnetic resonance and spin wave resonance has been presented for mixed magnetic phase materials. This theory can be adapted for any type of material and structure. The case of multilayered magnetic structures has not been discussed since it has been treated by other authors, where the results give resonance positions for various spin wave resonance modes that are in good agreement with other models [16–18, 45–47]. We find that in the ferromagnetic resonance limit our analysis shows agreement with previous authors [31].

We discuss in detail the system of random grain distribution of one magnetic phase in another. The nature of the morphology of the phases is very important to the nature of the spin wave resonances which may result. Although this may present problems of definition for the spin wave resonance, by making some simplifying assumptions the theory can accommodate these types of material. We demonstrate the importance of grain size and shape in the determination of the wavevector of standing spin wave resonance modes. We also discuss the effect of grain shape and spread in average grain size on the linewidth of the resonance lines, which also applies to interlayer roughness in the case of magnetic multilayers.

In the case of a purely ferromagnetic resonance response, the nature of the clustering of the magnetic phases no longer presents any difficulties, as the resonance would have a quasi-single phase type resonance equation, which effectively averages over the magnetic phases present in the sample. For the case of non-interacting magnetic phases the theory will predict resonances as expected for isolated magnetic phases. In the case of intermediate coupling it is necessary to solve the fourth-order equation in H.

Acknowledgments

We would like to thank the Spanish CICYT for financial support under research grant MAT96-1023. One of the authors, DSS, would also like to acknowledge the financial support of the Basque government.

Appendix A. Equations of motion in component form for a two phase system

From equations (15) and (16), it can be shown that the equation of motion can be written in component form as;

$$\left\{\frac{\mathrm{i}\omega}{\gamma_A} - \frac{1}{M_{0A}\sin\vartheta_A}\frac{\partial^2 E}{\partial\vartheta_A\partial\phi_A}\right\}m_{\vartheta A} - \left\{\frac{1}{M_{0A}\sin^2\vartheta_A}\frac{\partial^2 E}{\partial\phi_A^2} + \frac{2A_A}{M_{0A}}k_A^2\right\}m_{\phi A} - \frac{1}{M_{0B}\sin\vartheta_B}\frac{\partial^2 E}{\partial\vartheta_B\partial\phi_A}m_{\vartheta B} - \frac{1}{M_{0B}\sin\vartheta_B\sin\vartheta_A}\frac{\partial^2 E}{\partial\phi_B\partial\phi_A}m_{\phi B} = 0 \qquad \text{(A1)}$$

$$\left\{\frac{1}{M_{0A}}\frac{\partial^2 E}{\partial \vartheta_A^2}+\frac{2A_A}{M_{0A}}k_A^2\right\}m_{\vartheta A}+\left\{\frac{\mathrm{i}\omega}{\gamma_A}+\frac{1}{M_{0A}\sin\vartheta_A}\frac{\partial^2 E}{\partial\phi_A\partial\vartheta_A}\right\}m_{\phi A}$$
$$+\frac{1}{M_{0B}}\frac{\partial^2 E}{\partial\vartheta_A\partial\vartheta_B}m_{\vartheta B}+\frac{1}{M_{0B}\sin\vartheta_B}\frac{\partial^2 E}{\partial\vartheta_A\partial\phi_B}m_{\phi B}=0 \tag{A2}$$

$$-\frac{1}{M_{0A}\sin\vartheta_A}\frac{\partial^2 E}{\partial\vartheta_A\partial\phi_B}m_{\vartheta A}-\frac{1}{M_{0A}\sin\vartheta_A\sin\vartheta_B}\frac{\partial^2 E}{\partial\phi_A\partial\phi_B}m_{\phi A}$$
$$+\left\{\frac{\mathrm{i}\omega}{\gamma_B}-\frac{1}{M_{0B}\sin\vartheta_B}\frac{\partial^2 E}{\partial\vartheta_B\partial\phi_B}\right\}m_{\vartheta B}$$
$$-\left\{\frac{1}{M_{0B}\sin^2\vartheta_B}\frac{\partial^2 E}{\partial\phi_B^2}+\frac{2A_B}{M_{0B}k_B^2}\right\}m_{\phi B}=0 \tag{A3}$$

$$\frac{1}{M_{0A}}\frac{\partial^2 E}{\partial\vartheta_A\partial\vartheta_B}m_{\vartheta A}+\frac{1}{M_{0A}\sin^2\vartheta_A}\frac{\partial^2 E}{\partial\phi_A\partial\vartheta_B}m_{\phi A}$$
$$+\left\{\frac{1}{M_{0B}}\frac{\partial^2 E}{\partial\vartheta_B^2}+\frac{2A_B}{M_{0B}}k_B^2\right\}m_{\vartheta B}+\left\{\frac{\mathrm{i}\omega}{\gamma_B}+\frac{1}{M_{0B}\sin\vartheta_B}\frac{\partial^2 E}{\partial\phi_B\partial\vartheta_B}\right\}m_{\phi B}=0. \tag{A4}$$

Appendix B. List of substitutions

Substitutions in equations (17) and (18) are:

$$D_N=\frac{2A_N}{M_{0N}} \qquad P_{NM}=\frac{1}{M_{0N}\sin\vartheta_N\sin\vartheta_M}\frac{\partial^2 E}{\partial\phi_N\partial\phi_M}$$
$$\Omega_N=\frac{\omega}{\gamma_N} \qquad Q_{NM}=\frac{1}{M_{0N}}\frac{\partial^2 E}{\partial\vartheta_N\partial\vartheta_M}$$
$$P_N=\frac{1}{M_{0N}\sin^2\vartheta_N}\frac{\partial^2 E}{\partial\phi_N^2} \qquad R_{NM}=\frac{1}{M_{0N}\sin\vartheta_N}\frac{\partial^2 E}{\partial\vartheta_N\partial\phi_M}$$
$$Q_N=\frac{1}{M_{0N}}\frac{\partial^2 E}{\partial\vartheta_N^2} \qquad R'_{NM}=\frac{1}{M_{0N}\sin\vartheta_N}\frac{\partial^2 E}{\partial\vartheta_M\partial\phi_N}$$
$$R_N=\frac{1}{M_{0N}\sin\vartheta_N}\frac{\partial^2 E}{\partial\vartheta_N\partial\phi_N}. \tag{B1}$$

Substitutions made in equation (21) are:

$$p=\frac{1}{2A_A}\left\{\frac{\partial^2 E_{int}}{\partial\vartheta_A^2}+2A_{AB}\frac{\partial_n M_{0B}}{M_{0B}}\right\}-\frac{\partial_n M_{0A}}{M_{0A}}$$
$$q=\frac{1}{2A_A}\frac{M_{0A}}{M_{0B}}\frac{\partial^2 E_{int}}{\partial\vartheta_A\partial\vartheta_B}$$
$$r=\frac{1}{2A_A}\left\{\frac{1}{\sin\vartheta_A}\frac{\partial^2 E_{int}}{\partial\vartheta_A\partial\phi_A}-\frac{\cos\vartheta_A}{\sin^2\vartheta_A}\frac{\partial E_{int}}{\partial\phi_A}\right\}$$
$$s=\frac{1}{2A_A}\frac{1}{\sin\vartheta_B}\frac{M_{0A}}{M_{0B}}\frac{\partial^2 E_{int}}{\partial\phi_B\partial\vartheta_A}$$
$$t=\frac{1}{2A_A}\frac{1}{\sin\vartheta_A}\frac{M_{0A}}{M_{0B}}\frac{\partial^2 E_{int}}{\partial\vartheta_B\partial\phi_A}$$
$$u=\frac{1}{2A_A}\left\{\frac{\cos\vartheta_A}{\sin\vartheta_A}\frac{\partial E_{int}}{\partial\vartheta_A}+\frac{1}{\sin^2\vartheta_A}\frac{\partial^2 E_{int}}{\partial\phi_A^2}+2A_{AB}\frac{\partial_n M_{0B}}{M_{0B}}\right\}-\frac{\partial_n M_{0A}}{M_{0A}}$$
$$v=\frac{1}{2A_A}\frac{1}{\sin\vartheta_A\sin\vartheta_B}\frac{M_{0A}}{M_{0B}}\frac{\partial^2 E_{int}}{\partial\phi_B\partial\phi_A}. \tag{B2}$$

These are the general pinning parameters for a two phase magnetic system.

Appendix C. Second derivatives of the free energy for a two phase system

Using the free energy given in equation (26), where the anisotropy is uniaxial and of the form

$$E_K^n(\vartheta_n, \phi_n) = K_n^u \sin^2\vartheta_n \cos^2\phi_n. \tag{C1}$$

Then the second derivatives with respect to the angles are found to be:

$$\begin{aligned}\frac{\partial^2 E}{\partial \vartheta_A^2} = V_A\{&M_{0A}H[\sin\vartheta_A \sin\Theta_H \cos(\Phi_H - \phi_A) + \cos\vartheta_A \cos\Theta_H] \\ &-4\pi M_{0A}^2(\cos^2\vartheta_A - \sin^2\vartheta_A) + 2K_A^u \cos^2\phi_A(\cos^2\vartheta_A - \sin^2\vartheta_A)\} \\ &+K_{AB}M_{0A}M_{0B}[\sin\vartheta_A \sin\vartheta_B \cos(\phi_A - \phi_B)\cos\vartheta_A \cos\vartheta_B]\end{aligned} \tag{C2}$$

$$\begin{aligned}\frac{\partial^2 E}{\partial \phi_A^2} = V_A\{&M_{0A}H \sin\vartheta_A \sin\Theta_H \cos(\Phi_H - \phi_A) + 2K_A^u \sin^2\vartheta_A(\sin^2\phi_A - \cos^2\phi_A)\} \\ &+K_{AB}M_{0A}M_{0B}\sin\vartheta_A \sin\vartheta_B \cos(\phi_A - \phi_B)\end{aligned} \tag{C3}$$

$$\begin{aligned}\frac{\partial^2 E}{\partial \vartheta_A \partial \phi_A} = V_A\{&M_{0A}H\cos\vartheta_A \sin\Theta_H \sin(\Phi_H - \phi_A) - 4K_A^u \sin\vartheta_A \cos\vartheta_A \sin\phi_A \cos\phi_A\} \\ &+K_{AB}M_{0A}M_{0B}\cos\vartheta_A \sin\vartheta_B \sin(\phi_A - \phi_B).\end{aligned} \tag{C4}$$

Those derivatives with respect to θ_B and ϕ_B are found by interchanging the A and B subscripts. For the cross-derivative terms, we need only take the derivatives from the interaction energy, given in equation (28), as other terms will vanish, thus we find:

$$\frac{\partial^2 E}{\partial \vartheta_A \partial \vartheta_B} = -K_{AB}M_{0A}M_{0B}[\cos\vartheta_A \cos\vartheta_B \cos(\phi_A - \phi_B) + \sin\vartheta_A \sin\vartheta_B] = \frac{\partial^2 E}{\partial \vartheta_B \partial \vartheta_A} \tag{C5}$$

$$\frac{\partial^2 E}{\partial \phi_A \partial \phi_B} = -K_{AB}M_{0A}M_{0B}\sin\vartheta_A \sin\vartheta_B \cos(\phi_A - \phi_B) = \frac{\partial^2 E}{\partial \phi_B \partial \phi_B} \tag{C6}$$

$$\frac{\partial^2 E}{\partial \vartheta_A \partial \phi_B} = -K_{AB}M_{0A}M_{0B}\cos\vartheta_A \sin\vartheta_B \sin(\phi_A - \phi_B) = \frac{\partial^2 E}{\partial \phi_B \partial \vartheta_A} \tag{C7}$$

$$\frac{\partial^2 E}{\partial \vartheta_B \partial \phi_A} = K_{AB}M_{0A}M_{0B}\sin\vartheta_A \cos\vartheta_B \sin(\phi_A - \phi_B) = \frac{\partial^2 E}{\partial \phi_A \partial \vartheta_B}. \tag{C8}$$

References

[1] Grünberg P, Schrieber R, Pang Y, Walz U, Brodsky M B and Sowers H 1987 *J. Appl. Phys.* **61** 3756
[2] Baibich M N, Broto J M, Fert A, Nguyen Van Dan F, Petroff F, Etienne P, Creuzet G, Freiderich A and Chazelas J 1988 *Phys. Rev. Lett.* **61** 2472
[3] Parkin S S P, More N and Roche K P 1990 *Phys. Rev. Lett.* **64** 2304
[4] Unguris J, Celotta R J and Pierce D T 1991 *Phys. Rev. Lett.* **67** 140
[5] Herzer G 1989 *IEEE Trans. Magn.*, **25** 3327
[6] Yoshizawa Y, Oguma S and Yamauchi K 1988 *J. Appl. Phys.* **64** 6044
[7] Herzer G 1993 *Phys. Scr.* T **49** 307
[8] Slawska-Waniewska A, Nowicki P, Lachowicz H K, Gorria P, Barandiarán J M and Hernando A 1994 *Phys. Rev.* B **50** 6465
[9] Carbone C and Alvadaro S F 1987 *Phys. Rev.* B **36** 2433
[10] Fert A, Barthélémy A, Etienne P, Lequien S, Loloee R, Lottis D K, Mosca D H, Petroff F, Pratt W P and Schroeder P A 1992 *J. Magn. Magn. Mater.* **104–107** 1712
[11] Rührig M, Schäfer R, Hubert A, Mosler R, Wolf J A, Demokritov S and Grünberg P 1991 *Phys. Status Solidi* a **125** 635
[12] Grünberg P, Demokritov S, Fuss A, Schrieber R, Wolf J A and Purcell S T 1992 *J. Magn. Magn. Mater.* **104–107** 1734

[13] Bruno P and Chappert C 1991 *Phys. Rev. Lett.* **67** 1602
[14] Coehoorn R 1991 *Phys. Rev.* B **44** 9331
[15] Slonczewski J C 1995 *J. Magn. Magn. Mater.* **150** 13
[16] Vohl M, Barnas' J and Grünberg P 1989 *Phys. Rev.* B **39** 12 003
[17] Hillebrands B 1990 *Phys. Rev.* B **41** 530
[18] Puszkarski H 1992 *Phys. Rev.* B **46** 8926
[19] Mercier D and Lévy J-C S 1995 *J. Magn. Magn. Mater.* **139** 240
[20] Cochran J F 1995 *J. Magn. Magn. Mater.* **147** 101
[21] Schmool D S, Whiting J S S, Chambers A and Wilinska E A 1994 *J. Magn. Magn. Mater.* **131** 385
[22] Siruguri V and Kaul S N 1992 *J. Phys.: Condens. Matter* **4** 505
[23] Kaul S N and Mohan C V 1992 *J. Appl. Phys.* **71** 6090 and 6103
[24] Siruguri V and Kaul S N 1996 *J. Phys.: Condens. Matter* **8** 4545
Siruguri V and Kaul S N 1996 *J. Phys.: Condens. Matter* **8** 4567
[25] Schmool D S, Garitaonandia J S, Gorria P and Barandiarán J M 1997 unpublished
[26] Schmool D S and Barandiarán J M *J. Magn. Magn. Mater.* at press
[27] Berkowitz A E, Mitchell J R, Carey M J, Young A P, Zhang S, Spada F E, Parker F T, Hutten A and Thomas G 1992 *Phys. Rev. Lett.* **68** 3745
[28] Schmool D S, Garitaonandia J S and Barandiarán J M 1998 *Phys. Rev.* B at press
[29] Heinrich B, Purcell S T, Dutcher J R, Urquhart K B, Cochran J F and Arrott A S 1988 *Phys. Rev.* B **38** 12 879
[30] Cochran J F, Rudd J, Muir W B, Heinrich B and Celinski Z 1990 *Phys. Rev.* B **42** 508
[31] Layadi A and Artman J O 1990 *J. Magn. Magn. Mater.* **92** 143
[32] Schmool D S 1994 *DPhil Thesis* York
[33] Zhang Z, Zhou L, Wigen P E and Ounadjela K 1994 *Phys. Rev.* B **50** 6094
[34] Garitaonandia J S, Schmool D S and Barandiarán J M 1998 *Phys. Rev.* B at press
[35] Maksymowicz A Z 1986 *Phys. Rev.* B **33** 6045
[36] Iida S 1963 *J. Phys. Chem. Solids* **24** 625
[37] Smit J and Beljers H G 1955 *Philips Res. Rep.* **10** 113
[38] Rado G T and Weertman J R 1959 *J. Phys. Chem. Solids* **11** 314
[39] Pashaev Kh M and Mills D L 1991 *Phys. Rev.* B **43** 1187
[40] Barnas J 1991 *J. Magn. Magn. Mater.* **102** 319
[41] Cochran J F and Heinrich B 1992 *Phys. Rev.* B **45** 13 096
[42] Orúe I, Gorria P, Plazaola F, Fernández-Gubieda M L and Barandiarán J M 1994 *Hyperfine Interact.* **94** 2199
[43] Gorria P 1996 *PhD Thesis* Bilbao
[44] Skrotskii G V and Kurbatov L V 1966 *Ferromagnetic Resonance* ed S V Vonsovskii (Oxford: Pergamon)
[45] Barnas J and Grünberg P 1989 *J. Magn. Magn. Mater.* **82** 186
[46] Puszkarski H 1992 *Phys. Status Solidi* b **171** 205
[47] Jackson M, Mercier D, Levy J C S and Whiting J S S 1997 *J. Magn. Magn. Mater.* **170** 22
[48] Gorria P, Garitaonandia J S and Barandiarán J M 1996 *J. Phys.: Condens. Matter* **8** 5925